Technology Explanation

Analytical Technology for Axial Piston Pumps and Motors

SATO Naoto

Abstract

Axial piston pumps and motors are key products of our company, and are subject to various requirements from vehicle manufacturers such as greater speed, higher pressure, higher efficiency, smaller size and lower cost. In order to meet these requirements, various techniques are being devised such as reducing pressure loss by optimizing pump or motor part shape, reducing loss torque by improving rotating and sliding sections, and changing the oil path structure.

In analysis technology for pump and motor characteristics, on the other hand, progress has been made for some time in improving prediction technology by carrying out analysis taking into account the movement of rotary parts. This analysis technology is used to predict torque when starting and in the low speed range. However, for the prediction of pump and motor efficiency in the high speed range, there are points where verification of the detailed analysis model has not been sufficient. Also, conventional analysis technology has had issues with greater complexity of the sliding section structure (spherical surface) and switching to a two-segment structure of the outlet port (split flow type).

In this paper, analysis technology for piston pump and motor characteristics, effective for the high-speed range, was developed to support various product specifications. In addition, validity was confirmed through experimental verification. This analysis technology has been deployed as a standard tool for design inside our company, and is routinely utilized for pump and motor development.

1 Introduction

Axial piston pumps and motors (hereinafter referred to as "piston pumps and motors" or independently "pumps" and "motors") are the key products of KYB Corporation and widely used in construction machinery, industrial vehicles and agricultural machinery. Manufacturers of these vehicles or machinery demand various requirements for piston pumps and motors, such as higher speed, higher pressure, higher efficiency, smaller size and lower cost. In order to meet these requirements, KYB has conducted many different improvements, including making the sliding sections of the valve plate spherical and switching into a two-segment structure of the outlet port (split flow type).

In analysis technology for the piston pumps and motors, on the other hand, design of the rotary part consisting of a cylinder block (hereinafter C/B), which forms the basis of the product, and pistons is the key issue. The rotary part has three major sliding sections between:

① C/B and valve plate
② C/B and piston
③ Swash plate and piston shoe

The characteristics of these three sections affect the pump and motor performance. Particularly the C/B is substantially affected by all the three sliding sections above. Establishing behavior prediction technology in implementing the optimal design of the rotary part is indispensable.

KYB has conventionally conducted analyses on C/B behavior (hereinafter "C/B hydraulic balance analysis") and calculation of cylinder internal pressure, and effectively used these results for development of pumps and motors. Particularly scenes arise in which prediction of the C/B behavior or efficiency in the high speed region is required with the recent demand for higher speed and higher efficiency. The conventional C/B hydraulic balance analysis, however, usually covered prediction of starting torque or driving torque at low speeds and was not sufficient enough to be applied to verification at the high speed region. In addition, improvements for implementing the spherical valve plate and split flow type stated above were also challenges.

Then KYB has established C/B hydraulic balance analysis technology to support various product specifications based on the conventional C/B hydraulic balance analysis calculation model. The following provides the overview and cases of analysis.

2 Analysis Target

2.1 Rotary Part

Fig. 1 shows the rotary part to be analyzed. The sliding section between the C/B and valve plate shown in Fig. 1 has a plane surface. It is generally possible to achieve higher speed, higher pressure and a more stable performance by modifying the sliding section into the spherical type [1]. The basic structure of the rotary part is shared by the pumps and motors. The pump rotates its drive shaft to cause the pistons to reciprocate, thereby enabling suction and discharge of oil. The motor, on the contrary, uses hydraulic power to rotate the drive shaft.

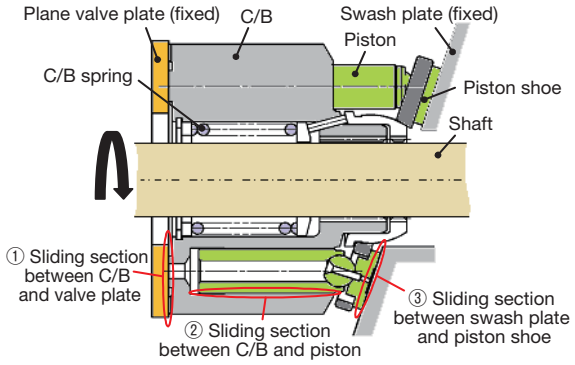

Fig. 1 Rotary part

2.2 Supporting Various Product Specifications

The design has been modified to support not only the two types of valve plates (plane and spherical) but also two types of flow: single flow and split flow. The single flow type here refers to the general flow construction with one suction port and one discharge port as shown in Fig. 2 (a). The split flow type has internal and external C/B ports (internal: blue, external: red) as shown in Fig. 2 (b), enabling two independent discharges.

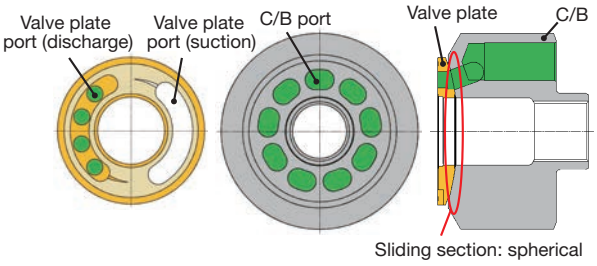

(a) Single flow type C/B, spherical valve plate port arrangement (for pumps)

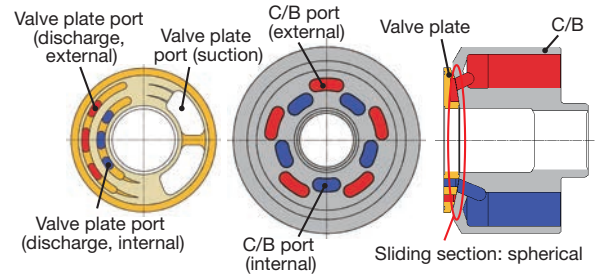

(b) Split flow type C/B, spherical valve plate port arrangement (for pumps)

Fig. 2 Construction of different flow types

3 C/B Hydraulic Balance

This chapter describes the hydraulic balance of the C/B, which is the basis of analysis.

The piston pump or motor contains the three major sliding sections as mentioned above. In particular, the sliding section between the C/B and valve plate is the critical part greatly affected by C/B behavior. It is necessary to minimize the leakage of hydraulic fluid from this sliding section and minimize friction and wear. To do so, C/B must be prevented from floating or inclining. It is also a must to avoid that C/B is pressed against the valve plate with excessive force. In other words, how to strike a dynamic balance of C/B is a critical issue.

To optimize the hydraulic balance of C/B, it is necessary to precisely identify the pressure distribution in the sliding section. Oil film pressure analysis is an effective approach to achieve this. The precision of the oil film pressure analysis depends on the precision of the modeling of the oil film profile in the sliding section. Therefore, how the oil film profile, which changes as C/B posture changes, can be modeled is important.

On the other hand, KYB has recently promoted development of a spherical valve plate, particularly that with a spherical diameter difference C_L, which is the difference between C/B spherical diameter S_c

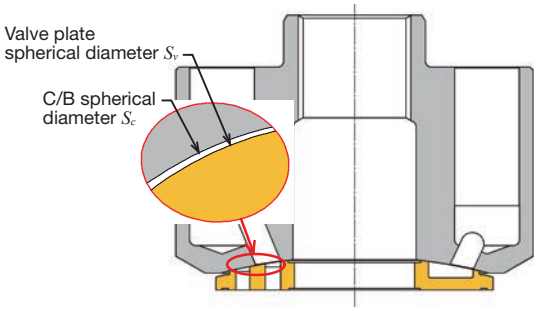

Fig. 3 Spherical diameter difference C_L ($=S_c-S_v$)

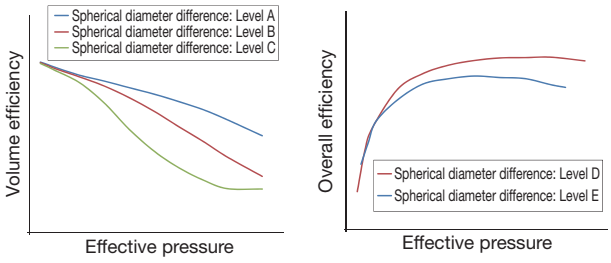

(a) Volume efficiency (b) Overall efficiency

Fig. 4 Effect of spherical diameter difference C_L

and the valve plate spherical diameter S_v ($C_L = S_c - S_v$, hereinafter "spherical diameter difference"). As an example, the results of tests on volume efficiency and overall efficiency on the effective pressure are shown in Fig. 4 (a) and (b) respectively. The findings that both the efficiencies greatly vary by the spherical diameter difference as shown in the figure imply how important the design of the spherical diameter difference is. However, the spherical diameter difference could not be taken into account in the conventional analysis approach based on the assumption that C/B and the valve plate had the same spherical diameter ($S_c = S_v$). This new analysis approach has introduced a modeling scheme for the oil film profile with the spherical diameter difference taken into account, thereby enabling evaluation of the possible effect of the difference.

4 Analysis Approach

4.1 Major Assumptions

This analysis approach uses the major assumptions:

- Only the shaft is deformable and all the other parts are solid.
- Only the three sections listed below are considered as sliding sections:
  ① Between C/B and valve plate
  ② Between C/B and piston
  ③ Between swash plate and piston shoe.
  Wear in any other parts is ignored.
- The mass of all parts is ignored.

4.2 Oil Film Pressure Analysis

The profile of the oil film in the sliding sections (① Between C/B and valve plate, ② Between C/B and piston, and ③ Between swash plate and piston shoe) is determined from the posture of C/B, pistons and piston shoes. Each of the oil film profiles is applied with the Reynolds Equation and the oil film pressure distribution is calculated using the finite element method (or the finite difference method). From the obtained oil film pressure distribution, the force, moment and leak rate are calculated.

As an example of the oil film profile, the following explains the sliding section between C/B and spherical valve plate with a spherical diameter difference. Aside from the overall coordinate system with its origin point O located at the spline center of the spline coupling between C/B and shaft shown in Fig. 5 (a), another local spherical surface coordinate system with its origin point located at the spherical surface center O_v of the spherical valve plate (spherical diameter S_v) is assumed. With the zenithal angle θ_v and the azimuthal angle φ_v, the spherical surface center O_c of C/B (spherical diameter S_c) is set to (e, θ_v', φ_v') as shown in Fig. 5 (b). This decides the geometry of C/B and the valve plate. Since $e \ll S_v/2$, oil film thickness h can be approximately expressed in the equation [2]:

$$h = C_L + e\sin\theta_v \sin\theta_v' \cos(\varphi_v - \varphi_v') + e\cos\theta_v \cos\theta_v' \quad (1)$$

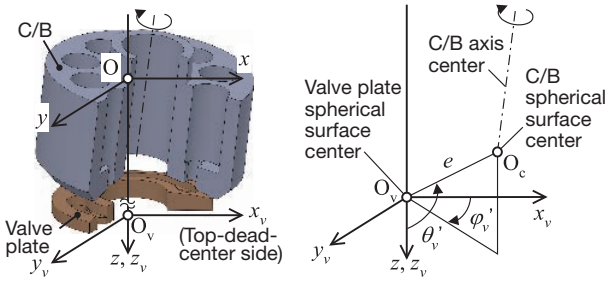

(a) Spherical surface coordinate system (b) Spherical surface center of C/B and valve plate

Fig. 5 Geometry of C/B and valve plate (for spherical valve plate)

The oil film profile of the split flow type determined from this analysis and the pressure distribution are shown in Fig. 6 (a) and Fig. 6 (b) respectively. According to Fig. 6 (a), oil film thickness h varies by the position of the sliding surface, although the figure is somewhat exaggerated in the direction of thickness. Force $\overrightarrow{F_{vp}}$ and moment $\overrightarrow{M_{vp}}$, which both depend on the oil film pressure distribution in the sliding section, can be calculated from the pressure distribution shown in Fig. 6 (b). The arrows shown in the figure indicate the magnitude and direction of moments M_{vpx} and M_{vpy} around the x and y axes in red for a positive value, or in blue for a negative value.

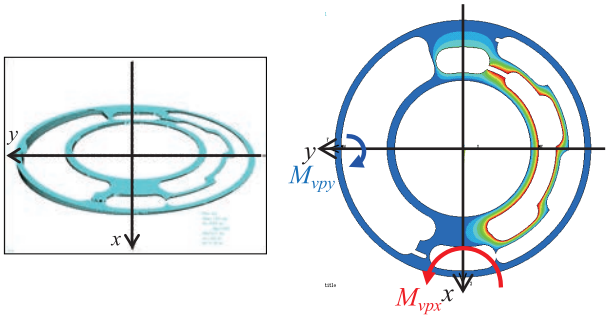

(a) Example of oil film profile (b) Example of pressure distribution

Fig. 6 C/B-valve plate sliding section (for spherical valve plate)

4.3 Shaft Elastic Deformation Analysis

In the Cartesian coordinate system with its origin point O located at the spline center as shown in Fig. 7, the shaft

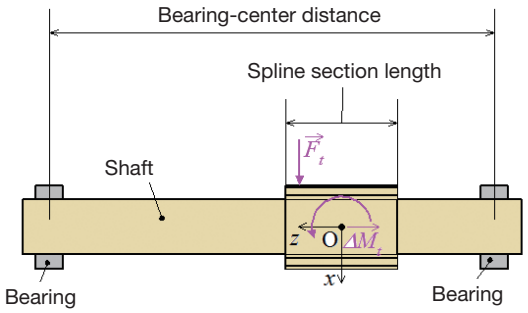

Fig. 7 Forces applied to shaft

is assumed to be a beam supported by bearings. The shaft deflection is calculated from C/B reaction force at spline coupling $\overrightarrow{F_t}$ and reaction moment $\Delta\overrightarrow{M_t}$. The interface between C/B and the shaft includes a clearance for the spline coupling.

4.4 C/B Posture Analysis

The forces applied to C/B are shown in Fig. 8. These forces can be roughly divided into four groups: the resultant of forces applied to the C/B cylinder section ($\overrightarrow{F_{CB}}$), forces applied to the C/B valve plate section (force due to oil film pressure distribution $\overrightarrow{F_{vp}}$, contact force caused by unbalanced forces $\overrightarrow{F_{vm}}$, and force caused by friction $\overrightarrow{F_{\mu v}}$), forces applied by the shaft ($-\overrightarrow{F_t}$) and forces applied by C/B spring (F_k). The resultant of forces applied to C/B cylinder section $\overrightarrow{F_{CB}}$ is the total sum of the forces of all the pistons. With the inertia force applied to C/B ignored, the four groups of forces above and the moment balance around the origin point O can be expressed in the equations: [3].

$$\left.\begin{aligned} F_{CBx}+F_{vpx}+F_{vmx}+F_{\mu vx}-F_{tx}&=0\\ F_{CBy}+F_{vpy}+F_{vmy}+F_{\mu vy}-F_{ty}&=0\\ F_{CBz}+F_{vpz}+F_{vmz}+F_{\mu vz}-F_{tz}+F_k&=0 \end{aligned}\right\} \quad (2)$$

$$\left.\begin{aligned} M_{CBx}+M_{vpx}+M_{vmx}+M_{\mu vx}-M_{tx}&=0\\ M_{CBy}+M_{vpy}+M_{vmy}+M_{\mu vy}-M_{ty}&=0\\ M_{CBz}+M_{vpz}+M_{vmz}+M_{\mu vz}-M_{tz}&=0 \end{aligned}\right\} \quad (3)$$

where the terms in Equation (3) are the components around the axes of moment $\overrightarrow{M_{CB}}$, $\overrightarrow{M_{vp}}$, $\overrightarrow{M_{vm}}$, $\overrightarrow{M_{\mu v}}$ and $-\overrightarrow{M_t}$ generated by $\overrightarrow{F_{CB}}$, $\overrightarrow{F_{vp}}$, $\overrightarrow{F_{vm}}$, $\overrightarrow{F_{\mu v}}$, $-\overrightarrow{F_t}$ and $\Delta\overrightarrow{M_t}$.

C/B posture is calculated so as to satisfy Equations (2) and (3) above.

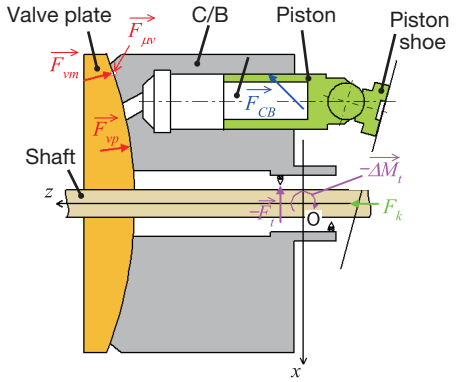

Fig. 8 Forced applied to C/B

4.5 C/B Hydraulic Balance Analysis Procedure

Fig. 9 gives a flowchart of analysis on C/B hydraulic balance. After initial conditions are set, analysis on the oil film pressure for each C/B rotation angle, analysis on the shaft elastic deformation and analysis on C/B posture are repeated to provide convergent calculation of C/B posture. This set of calculations are conducted for each increase $\Delta\theta$ in C/B rotation angle until reaching one pitch (= result of 360 degrees divided by the number of pistons n). The various efficiencies are calculated from the leak rate for the pitch of C/B rotation angle and the average of lost torque.

5 Analysis Cases

5.1 Target Products

The target product of this analysis case is 1C/B piston pump PSVL2-42 for compact excavators [4] and is developed by using this analysis technology. Fig. 10 shows the appearance of PSVL2-42 and Table 1 provides the major specifications of PSVL2-42. This pump uses a spherical valve plate.

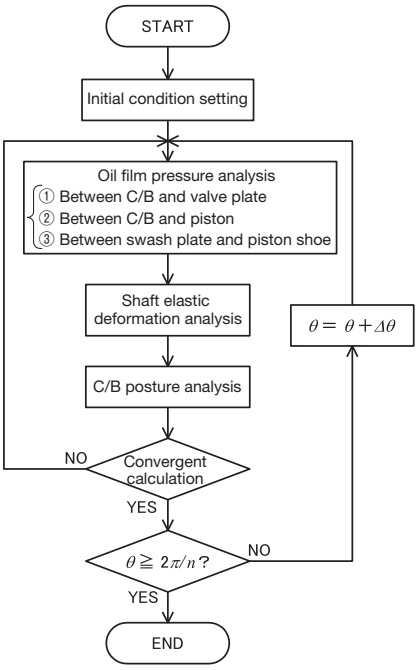

Fig. 9 C/B hydraulic balance analysis flowchart

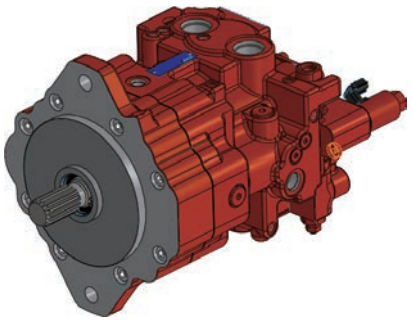

Fig. 10 PSVL2-42

Table 1 Major specifications of PSVL2-42

Displacement [cm^3/rev]	Split flow: 42.3 + 42.3
Max. pressure [MPa]	32
Max. speed [rpm]	2,200

5.2 Analysis Condition

(1) Friction coefficient of each sliding section

The coefficient of friction is determined for each sliding section from the findings accumulated in the company and the results of newly conducted tests. The coefficient of friction in each sliding section is given according to the rotation speed.

(2) Minimum oil film thickness in each sliding section

Minimum oil film thickness in each sliding section is determined from the findings accumulated in the company and the results of newly conducted tests.

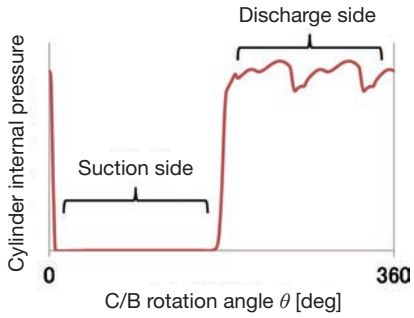

Fig. 11 Cylinder internal pressure calculation result (example)

(3) Cylinder internal pressure

Calculation results of the cylinder internal pressure prediction program, which is KYB's design standard tool, are used for hydraulic balance analyses. The program can take into account the effects of swash plate vibration, discharge pulsation, notch profile and other factors. Fig. 11 gives an example of the result of cylinder internal pressure calculation for the external C/B ports of PSVL2-42. The horizontal axis represents C/B rotation angle θ and the vertical axis represents cylinder internal pressure. For analysis on C/B hydraulic balance, pressure pulsation on the discharge side may be considered as shown in Fig. 11.

5.3 Examples of Analysis Results

(1) Pressure distribution in C/B-valve plate sliding section

Figs. 12 and 13 show the pressure distribution in the sliding section between C/B and valve plate by 20 degrees of C/B rotation angle when the internal and external ports have high pressure respectively. The two figures show that, in either case of the high pressure internal or external port, the moment around x axis M_{vpx} is always stable with positive values, while the moment around y axis M_{vpy} shows negative and positive values that may be reversed depending on C/B rotation angle θ. Since the internal and external ports have five pistons each, one pitch is 72 degrees.

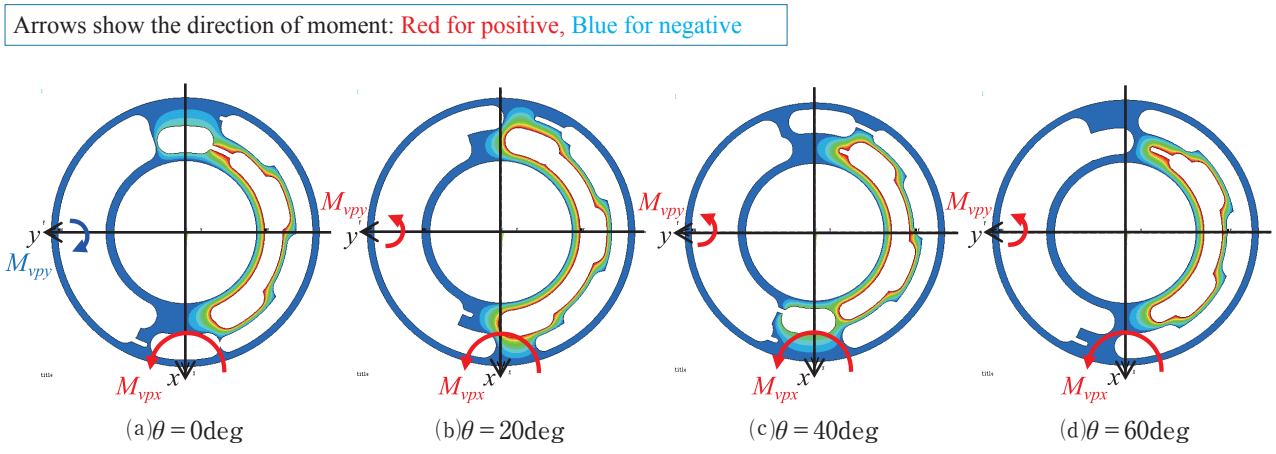

Fig. 12 Pressure distribution in C/B-valve plate sliding section (spherical diameter difference ①, high pressure internal port)

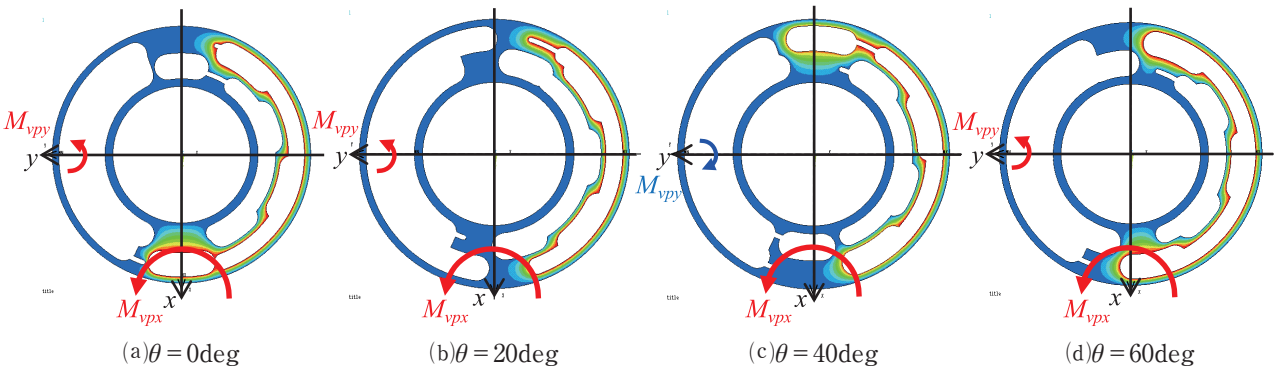

Fig. 13 Pressure distribution in C/B-valve plate sliding section (spherical diameter difference ①, high pressure external port)

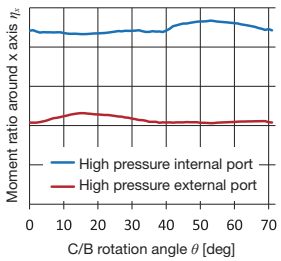

(a) Spherical diameter difference ①

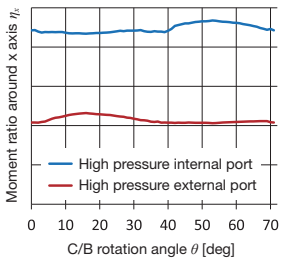

(b) Spherical diameter difference ②

Fig. 14 Moment ratio around x axis η_x

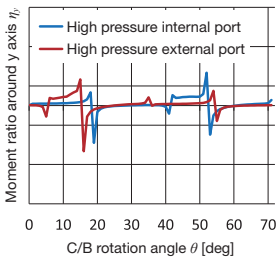

(a) Spherical diameter difference ①

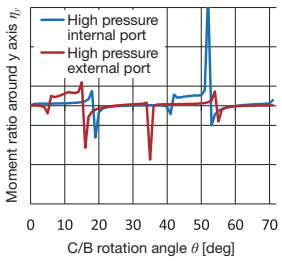

(b) Spherical diameter difference ②

Fig. 15 Moment ratio around y axis η_y

(2) Moment ratio

Moment ratio is one of the hydraulic balance design indexes. Moment ratio around the x and y axes applied to C/B can be respectively expressed using the equation:

$$\eta_x = -\frac{M_{CBx}}{M_{vpx}},\ \eta_y = -\frac{M_{CBy}}{M_{vpy}} \tag{4}$$

Figs. 14 and 15 show the moment ratio around the x and y axes for one pitch for two levels of spherical diameter difference respectively. The effect of the spherical diameter difference on the moment ratio around the x axis is small, while that on the moment ratio around the y axis is substantial depending on C/B rotation angle θ. This is probably because of the timing at which the moment around y axis M_{vpy} is switched between positive and negative values as stated in paragraph (1) above. Both moment ratios around the x and y axes should be designed so that the variation for one pitch can meet the design standard.

(3) Pressing ratio

Pressing ratio is one of the hydraulic balance design indexes and can be expressed as the ratio of loads applied to the C/B in the direction of the z axis using the equation:

$$\eta = -\frac{F_{CBz} + F_k}{F_{vpz}} \tag{5}$$

Fig. 16 shows the pressing ratio for a single pitch. In both the high pressure internal and external port cases, the pressing ratio substantially changes around C/B rotation angle θ = 0,40 degrees. These changes coincide with the timing of switching the number of high pressure pistons from two to three or three to two. Like the moment ratio, the pressing ratio should be designed so that the variation for one pitch can meet the design standard.

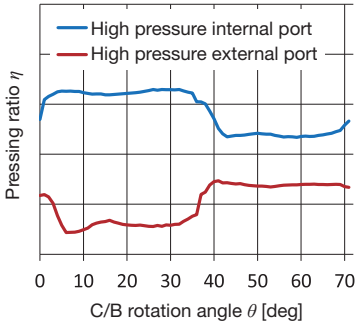

Fig. 16 Pressing ratio

5.4 Experimental Verification of Analysis Precision

To verify the analysis precision, tests using actual machines were conducted for the two levels of the spherical diameter difference shown in Figs. 14 and 15. The relationship between the discharge pressure obtained from the actual machine tests and various efficiencies was compared to the analysis result as shown in Fig. 17. In the figure, a solid line indicates analysis results and a broken line indicates actual measurements. For volume efficiency, the high pressure external port case shows lower efficiency compared to the high pressure internal port case for both analysis and measurement, which is more obvious with spherical diameter difference ② than with spherical diameter difference ①. For mechanical efficiency, no substantial difference is seen between the high pressure external and internal port cases, or between the two levels of spherical diameter difference. As a result, the overall efficiency is dominantly affected by the volume efficiency for both analysis and measurements. From the results above, the analysis results have a very similar tendency to that of the actual measurements. It can be concluded that this analysis technology can be used for qualitative prediction of the various efficiencies as an effective tool for design development.

6 Concluding Remarks

Technology to analyze C/B hydraulic balance has been established to support various product specifications (plane and spherical valve plates, single and split flow types) of piston pumps and motors. In addition, the appropriateness of the calculation results on the various efficiencies at a high speed region has been verified. This analysis technology has been introduced as an in-house design standard tool and is effectively used for achieving higher efficiency in pump/motor development or optimal design of products.

From now on we will discuss application of the mixed lubrication theory or the elasto-hydrodynamic lubrication theory to the sliding sections that are currently applied

with the hydrodynamic lubrication theory, in order to address quality issues including seizure and wear.

Finally, I would like to show my deep appreciation to those who extended their full cooperation to the establishment of the analysis technology.

Major symbols

C_L : Spherical diameter difference ($= S_c - S_v$)
h : Oil film thickness
n : Number of pistons
F_k : C/B spring force
$\overrightarrow{F_{CB}}$: Resultant of forces applied to C/B cylinder section. Components in the direction of axes (F_{CBx}, F_{CBy}, F_{CBz})
$\overrightarrow{F_t}$: Force applied by C/B to shaft. Components in the direction of axes (F_{tx}, F_{ty}, F_{tz})
$\overrightarrow{F_{vm}}$: Contact force caused by unbalanced forces between C/B and valve plate. Components in the direction of axes (F_{vmx}, F_{vmy}, F_{vmz})
$\overrightarrow{F_{vp}}$: Force due to the oil film pressure distribution between C/B and valve plate. Components in the direction of axes (F_{vpx}, F_{vpy}, F_{vpz})
$\overrightarrow{F_{\mu v}}$: Friction force between C/B and valve plate. Components in the direction of axes ($F_{\mu vx}$, $F_{\mu vy}$, $F_{\mu vz}$)
$\overrightarrow{M_{CB}}$: Combined moment related to the origin point O of forces applied to C/B cylinder section $\overrightarrow{F_{CB}}$. Components in the direction of axes (M_{CBx}, M_{CBy}, M_{CBz})
$\overrightarrow{M_t}$: Moment caused by force applied by C/B to shaft $\overrightarrow{F_t}$ and reaction moment $\overrightarrow{\Delta M_t}$. Components around axes (M_{tx}, M_{ty}, M_{tz})
$\overrightarrow{M_{vp}}$: Moment caused by force $\overrightarrow{F_{vp}}$ due to the oil film pressure distribution applied to C/B valve plate section. Components around axes (M_{vpx}, M_{vpy}, M_{vpz})
$\overrightarrow{M_{vm}}$: Moment caused by contact force $\overrightarrow{F_{vm}}$ resulting from unbalanced forces applied to C/B valve plate section. Components around axes (M_{vmx}, M_{vmy}, M_{vmz})
$\overrightarrow{M_{\mu v}}$: Moment caused by friction force $\overrightarrow{F_{\mu v}}$ applied to C/B valve plate section. Components in the direction of axes ($M_{\mu vx}$, $M_{\mu vy}$, $M_{\mu vz}$)
$\overrightarrow{\Delta M_t}$: Reaction moment applied by C/B to shaft. Components in the direction of axes (ΔM_{tx}, ΔM_{ty}, ΔM_{tz})
e, θ_v', φ_v': Coordinate of C/B spherical surface center
O_c : C/B spherical surface center
O_v : Spherical surface center of spherical valve plate
S_c : C/B spherical diameter
S_v : Valve plate spherical diameter
η : Pressing ratio
η_x, η_y : Moment ratio around x and y axes
θ : C/B rotation angle
$\Delta\theta$: Increase in C/B rotation angle used during C/B hydraulic balance analysis
θ_v : Zenithal angle
φ_v : Azimuthal angle

References

1) Japan Fluid Power Association: Oil Hydraulics-Handbook (2012 edition).
2) YAMAGUCHI, SHIMIZU: Comparison of Spherical Valve Plates with Plane Valve Plates from the Viewpoint of Film Lubrication for Piston Pumps. Hydraulics and pneumatics, Vol. 20, No.2 (1989).

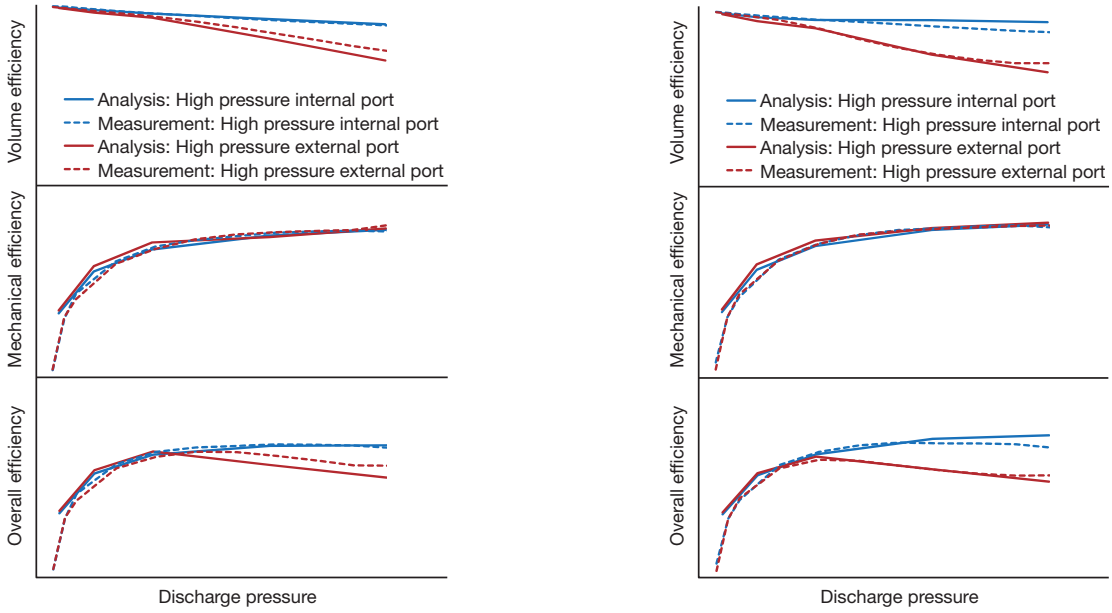

(a) Spherical diameter difference ①　　(b) Spherical diameter difference ②

Fig. 17 Example of efficiency precision verification (piston pump)

3) YAMAGUCHI: Formation of a Fluid Film Between a Valve Plate and a Cylinder Block of Piston Pumps and Motors, 1st Report, Valve Plate with Dynamic Pad, Transactions of the Japan Society of Mechanical Engineers (JSME), Series B, Vol.51, No.469 (1985).
4) TAKEI, SAKAI: Development of Piston Pumps for Compact-Excavators, KYB Technical Review No. 54 (2017).

Author

SATO Naoto

Joined the company in 1999.
Sagami Office, CAE Improvement Dept., Engineering Div.
Ph.D (engineering).
Engaged in analysis on various products.